Androgen receptor targeted conjugate for bimodal photodynamic therapy of prostate cancer in vitro

Journal:	*Bioconjugate Chemistry*
Manuscript ID:	bc-2015-002616.R1
Manuscript Type:	Article
Date Submitted by the Author:	18-Jun-2015
Complete List of Authors:	Varchi, Greta; CNR-ISOF, Rapozzi, Valentina; University of Udine, Biomedical Science and Technology Ragno, Daniele; Università di Ferrara, Chemical and Pharmaceutical Sciences Castoria, Gabriella; II University of Naples, Department of Biochemistry, Biophysics and General Pathology DI DONATO, marzia; Second University of Naples, Della Pietra, Emilia; University of Udine, Biomedical Science and Technology Benfenati, Valentina; Italian National Reserach Council, Institute of Organic Chemistry and Photoreactivity Ferroni, Claudia; Consiglio Nazionale delle Ricerche, Istituto per la Sintesi Organica e la Fotoreattività Guerrini, Andrea; Consiglio Nazionale delle Ricerche, Istituto per la Sintesi Organica e la Fotoreattività Cesselli, Daniela; University of Udine, Department of Biomedical Science and Technology Saracino, Emanuela; Italian National Research Council, e.saracino@bo.ismn.cnr.it

Androgen receptor targeted conjugate for bimodal photodynamic therapy of prostate cancer in vitro

Valentina Rapozzi,[‡] Daniele Ragno,[∫] Andrea Guerrini,[†] Claudia Ferroni,[†] Emilia della Pietra,[‡] Daniela Cesselli,[‡] Gabriella Castoria,[§] Marzia Di Donato,[§] Emanuela Saracino,[£] Valentina Benfenati,[†] and Greta Varchi*[†]

† Institute of the Organic Synthesis and Photoreactivity Italian National Research Council
Via P. Gobetti, 101 40129 Bologna – IT E-mail: greta.varchi@isof.cnr.it

‡ Department of Medical and Biological Sciences University of Udine Piazzale Kolbe, 4 – 33100 Udine – IT

∫ Department of Chemistry University of Ferrara Via Fossato di Mortara, 17 - 44121 Ferrara – IT

§ Department of Biochemistry, Biophysics and General Pathology – II University of Naples
Via L. De Crecchio, 7 -80138 Naples – IT

£ Institute for the Study of Nanostructured Materials Italian National Research Council
Via P. Gobetti, 101, 40129 Bologna – IT

*Correspondence should be addressed to:
Greta Varchi, PhD, Institute of Organic Synthesis and Photoreactivity, Italian National Research Council, Via Gobetti, 101, 40129 Bologna, Italy. Phone: +39 0516398283; Fax +39 0516398349; E-mail: greta.varchi@isof.cnr.it.

Abstract

Prostate cancer (PC) represents the most common type of cancer among males and is the second leading cause of cancer death in men in Western society. Current options for PC therapy remain unsatisfactory, since they often produce uncomfortable long-term side effects, such as impotence (70%) and incontinence (5-20%) even in the first-stages of the disease. Light-triggered therapies, such as photodynamic therapy, have the potential to provide important advances in the treatment of localized and partially metastasized prostate cancer. We have designed a novel molecular conjugate (**DR2**) constituted of a photosensitizer (pheophorbide *a*, Pb*a*), connected to a non-steroidal antiandrogen molecule through a small pegylated linker.

This study aims at investigating whether **DR2** represents a valuable approach for PC treatment based on light-induced production of single oxygen and nitric oxide (NO) *in vitro*. Besides being able to efficiently bind the androgen receptor (AR), the 2-trifluoromethylnitrobenzene ring on the **DR2** backbone is able to release cytotoxic NO under the exclusive control of light, thus augmenting the general photodynamic effect. Although **DR2** is similarly internalized in cells expressing different levels of androgen receptor, the AR ligand prevents its efflux through the ABCG2-pump. *In vitro* photo-toxicity experiments demonstrated the ability of **DR2** to kill cancer cells more efficiently than Pb*a*, while no dark-toxicity was observed. Overall, the presented approach is very promising for further development of AR-photosensitizer conjugates in the multi-modal photodynamic treatment of prostate cancer.

Introduction

Prostate cancer (PC) is the leading cause of cancer death for men in Western countries and an emerging malignancy in developing nations.[1] Depending on the diagnosis response, PC treatment options vary. Clinicians may decide for an active surveillance or for more invasive treatments such as surgical removal of the prostate gland, external or internal radiotherapy alone or in combination with androgen depletion therapy (ADT). Despite being effective in shrinking tumor burden and improving survival, these therapies frequently fail and castration-resistant prostate cancer (CRPC) frequently develops.[2] At this stage, PC is almost incurable and often accompanied by metastatic spreading and poor prognosis, with a median survival range from 12 to 24 months.[3] Unfortunately, few biomarkers predictive of metastatic phenotype have been identified yet and few therapeutic options are available for CRPC patients. Although chemotherapy remains the first choice of most clinicians at this stage, its overall benefit is very modest, since PC frequently escapes from chemotherapy at both primary and metastatic sites.[4–6] Within the past years, several promising agents, including inhibitors of androgen synthesis or androgen receptor (AR) activation have improved CRPC patient survival.[7–9] Nevertheless, CRPC has evolved mechanisms to reactivate AR despite continued ADT. Therefore, further progress, beyond the discovery of more potent and selective drugs, is strongly warranted. The multi-modal treatment involving the administration of different therapeutic agents acting synergistically and/or in combination with techniques has emerged as a successful approach.[10] In this context, light-triggered therapies, such as photodynamic therapy (PDT), have the potential to provide important advances in the treatment of localized and partially metastasized PC. PDT consists of three essential components: a photosensitizer (PS), light and oxygen that together initiate a photochemical reaction that culminates in the generation of highly reactive oxygen species (ROS) responsible of tumor cells death.[11] Indeed, in June 2013 Tookad® has entered a randomized phase III clinical trial for vascular targeted PDT of localized PC (https://clinicaltrials.gov/ct2/show/NCT01875393?term=NCT01875393&rank=1). Interestingly, light can be delivered to the entire prostate gland and to near-by metastasized organs by using interstitial, cylindrically diffusing optical fibres.[12] Unlike chemotherapy or radiotherapy, the cell killing mechanism triggered by PDT is not directly dependent on DNA damage, thus decreasing the chances of therapy cross-resistance and eliminating late normal tissue effects such as second malignancy.[13]

Based on these preliminary considerations, we focused our study on the development of a novel tri-component conjugate composed of a bacteriochlorin (pheophorbide *a*, Pb*a*, Figure 1),[14] connected to a non-steroidal antiandrogen compound (Figure 1, **A**) through a small pegylated linker, with the aim of investigating *in vitro* whether this compound represents a valuable approach for the targeted multi-modal treatment of PC.

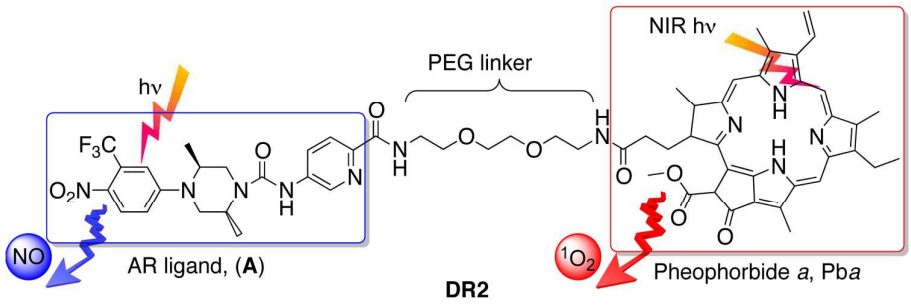

Figure 1. Chemical structure of conjugate **DR2**.

To this purpose, the synthetically modified 2,5-piperazine derivative **A** (Figure 1) was selected for (i) its high affinity to AR and ability to antagonize the receptor and (ii) the presence of the nitro substituent for the possible light-induced release of nitric oxide (NO). 2,5-piperazine derivatives represent potent orally and peripherally selective non-steroidal AR antagonists exhibiting high affinity for the AR.[15] In principle, these features could favor the overall activity of the conjugate by binding to the receptor following its internalization. Recently Dreaden and co-workers demonstrated that by binding to AR and the G-protein GPRC6A, antiandrogen-decorated gold nanoparticles exhibit enhanced therapeutic efficacy as compared to the reference drug.[16] Additionally, the conjugation of an antiandrogen moiety with a histone deacetylase inhibitor (HDACi) displays higher HDACi efficacy and selectivity in PC treatment as compared to HDACi alone.[17]

In recent years NO has stimulated a great deal of interest not only for its essential role in various biological functions,[18] but also for its promising anticancer activity.[19] NO levels in the tumor and its microenvironment can directly influence the response of cancer cells to PDT, confirming a pivotal role of exogenous NO in the overall antitumor PDT response.[20,21] As an example, the combination of the NO donor, DETANONOate, and PDT resulted in significant potentiation of the cytotoxic effect *in vitro* and *in vivo*.[22] Moreover, several research groups have recently developed novel NO donors to promote PDT-mediated anti-tumor cytotoxicity. For instance, Carneiro and co-workers reported the synthesis and activity of a nitrosyl-phtalocyanin ruthenium complex [Ru(NO)(NO)(ONO)(pc)] and studied its effect on a murine melanoma cell line, B16F10, in the presence or absence of light irradiation. Their findings demonstrated that the complex was more effective in inhibiting B16F10 cell growth than the [Ru (pc)], thereby confirming the importance of NO release in PDT treatment.[23]

Among small molecules, the ones bearing a 2-trifluoromethylnitrobenzene ring have been established as effective NO donors as they are able to generate nitric oxide through a nitro-to-nitrite photo-rearrangement that occurs upon controlled irradiation with light at 400 nm wavelength (Figure 2).[24,25]

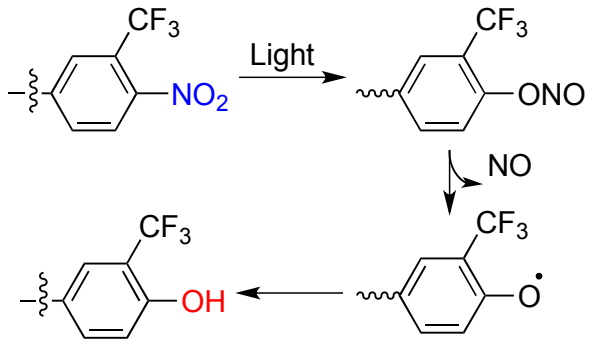

Figure 2. Light-induced NO-releasing mechanism of nitrobenzene compounds.

In this work we present *in vitro* findings obtained using the newly synthesized **DR2** molecular conjugate. In particular, the presented experiments focus on the ability of **DR2** to be efficiently internalized in different PC cell lines and to function as a multi-modal photosensitizer, thus being capable of generating ROS and NO upon light activation, thereby providing additive photo-toxicity.

Results and Discussion

Conjugates synthesis and characterization

Scheme 1 shows the synthesis of conjugate **DR2**. Acid **1** was obtained according to a slightly modified literature procedure[15,26] (see also Supporting Information for details) and reacted with N-hydroxy succinimide in presence of *N,N′*-Dicyclohexylcarbodiimide (DCC) in 1,4-dioxane to afford compound **2** in good yield. Derivative **2** was than coupled with N-Boc-2,2′ -(ethylene-1,2-dioxy)bis(ethylamine) in the presence of pyridine in tetrahydrofuran (THF), followed by deprotection of the amino group with CF_3COOH to provide compound **3** in quantitative yield. Coupling reaction between NHS-activated Pb*a* (**4**) and derivative **3** was carried out in the dark and in the presence of pyridine at room temperature to provide conjugate **DR2** in acceptable yield.

Scheme 1. Synthesis of conjugate **DR2**.[a]

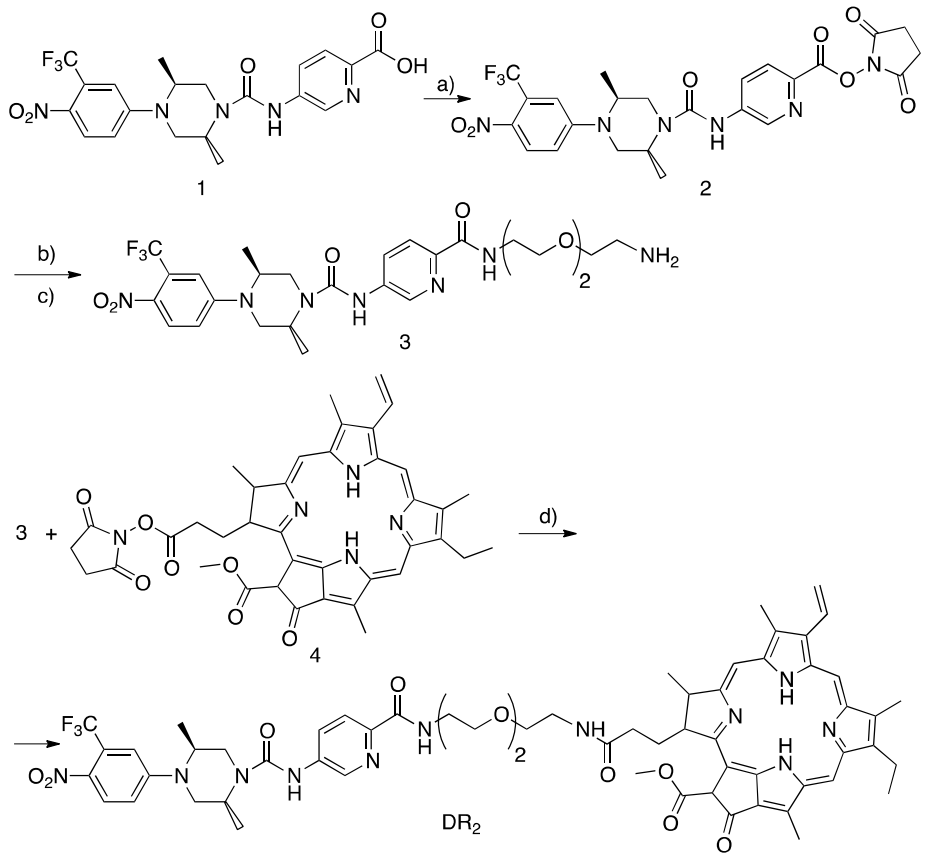

[a]Reaction conditions and reagents: a) DCC, NHS, 1,4-dioxane, rt, 5 h; (45%); b) H_2N-$[(CH_2)_2O]_2(CH_2)_2NH(CO)O^tBu$, Py, THF, rt, 21 h; (100%); c) CF_3COOH, rt, 2 h (46%); d) Py, THF, dark, rt, 22 h; (98%).

Whenever necessary intermediates and final compound were purified by silica gel column chromatography and characterized by ^1H and ^{13}C NMR, and HRMS.

The electronic absorption spectra of **DR2** was recorded in CH_2Cl_2 and compared with free Pb*a*. The spectra of the novel conjugate show the typical features of non-aggregated Pb*a* (Figures S1 in Supporting Information Section) and display a Soret band at 415 nm, slightly red-shifted with respect to Pb*a* alone (404 nm) and an intense Q band at 670 nm. A shoulder responsible for the absorption of the antiandrogen ligand is detected at 400 nm.

DR2 *displaces the androgen receptor ligand binding.*

We used the prostate cancer-derived LNCaP cells, since they represent a model to analyze the androgen-responsiveness and AR activation.[27] Using a siRNA approach, we firstly depleted LNCaP cells of AR and control cells were transfected with non-targeting siRNA. Transfected cells were made quiescent and then incubated with 10 nM of the synthetic AR radio-ligand [3H]-methyltrienolone ([^{3}H] R1881). Cells were collected and used for the ligand-binding assay. Results presented in Figure 3A show that the [^{3}H] R1881 binding decreases when AR was silenced. By increasing siRNA AR concentration (from 125 to 250 picomol, respectively), a parallel decrease (85% and 93%) in AR ligand binding was observed. The Western blot from lysate proteins (inset in Figure 3B), together with the densitometric analysis (Figure 3B) show that AR levels

decrease as siRNA AR concentration increases. Therefore, our assay is specific for AR expressed in LNCaP cells.

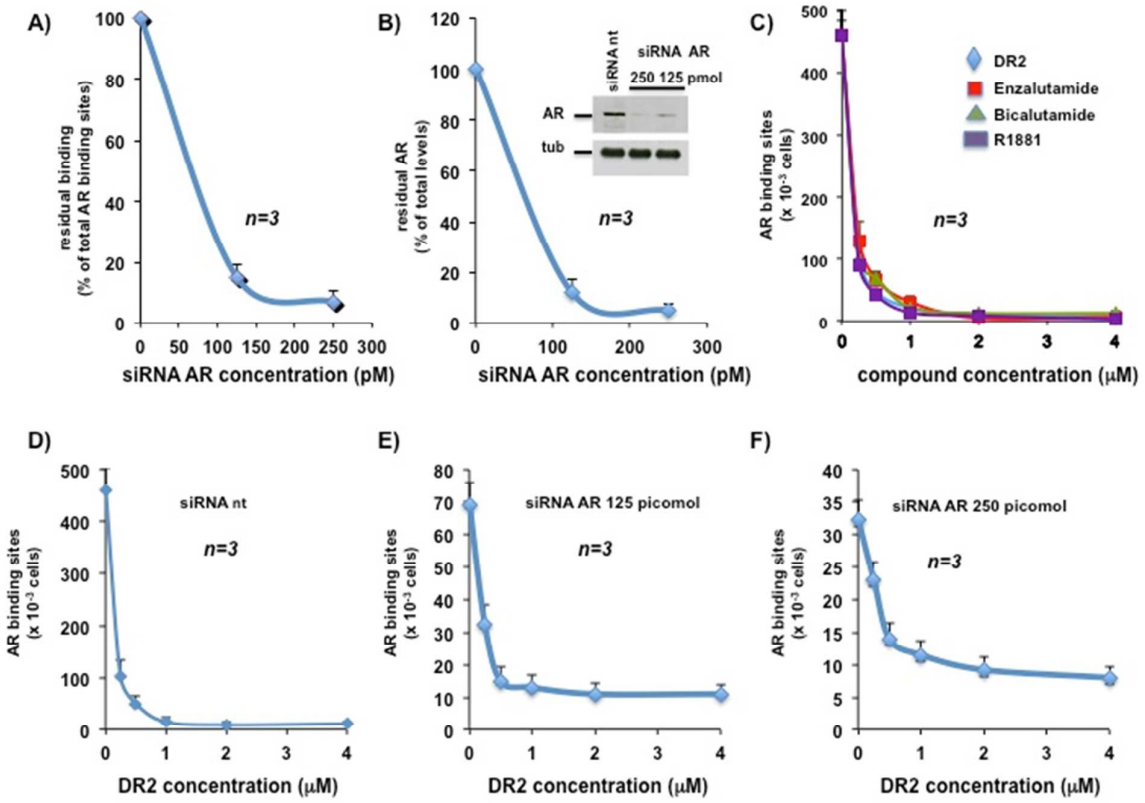

Figure 3. AR ligand binding displacement studies in LNCaP cells. **A)** LNCaP cells were transfected with siRNA nt (0 on x axis) or the indicated amounts of siRNA AR. Transfected cells were incubated with 10 nM [^{3}H] R1881. Intracellular radioactivity was assayed and residual binding was calculated and expressed as % of total AR binding sites. Inset in **B**, shows the Western blot of AR in the different experimental conditions. The membrane was stripped and re-probed with anti tubulin antibody, as a loading control. **B**) Densitometric analysis of Western blot is shown. AR levels were normalized for tubulin amounts. Residual AR was expressed as % of the total level, which corresponds to the receptor level detected in LNCaP cells transfected with siRNA nt. **C)** Quiescent LNCaP cells were incubated with 10 nM [^{3}H] R1881, in the absence or presence of the indicated excess (from 0 to 4 μM) of **DR2** or unlabeled R1881, or bicalutamide, or enzalutamide. Intracellular radioactivity was assayed and AR binding sites x 10^{-3} cells were calculated. **D)-F)** LNCaP cells were transfected with nt (**D**), or AR siRNAs (125 pM or 250 pM in **E** and **F**, respectively). Cells were incubated with 10 nM [^{3}H] R1881, in the absence or presence of the indicated excess (from 0 to 4 μM) of **DR2** Intracellular radioactivity was assayed and AR binding sites x 10^{-3} cells were calculated. In **D)-F)**, the different values on the y axis are due to the increase in siRNA AR concentration, and hence to the parallel decrease in AR binding sites. **A)-F)**, data were collected from three different experiments. Means and SEM are shown.

The efficacy of **DR2** in displacing the AR ligand binding activity was similar to that observed using unlabeled R1881, or bicalutamide, or enzalutamide, two non-steroidal antiandrogens largely used in PC treatment,[7] in LNCaP cells (Figure 3C). Again, a very significant [^{3}H] R1881 displacement was detected when the conjugate **DR2** was used at 0,25 and 0,5 μM in LNCaP cells transfected with non-targeting siRNA (Figure 3D). By increasing the **DR2** concentration (from 1 to 4 μM), an almost complete displacement of AR

ligand binding activity was detected (Figure 3D). Similar findings were observed by using unlabeled R1881 (at 1 μM). Bicalutamide or enzalutamide show a similar effect on AR ligand binding displacement when used at 1 μM (legend to Figure 3D). **DR2** was still able to displace the [^{3}H] R1881 binding in LNCaP cells depleted of different amounts of AR upon siRNA AR transfection (125 picomol and 250 picomol, respectively in Figure 3E and F).

In sum, these findings show that **DR2** specifically binds AR and is active in displacing the receptor ligand binding activity even when low AR amounts are expressed, as it often occurs in PC-associated fibroblasts.[28]

DR2 *in vitro uptake and internalization studies in AR-expressing PC cells.*

We then evaluated the **DR2** delivery/uptake in VCaP cells, which over-express the wild type AR.[29] The extent of conjugate uptake over time was quantified by fluorescence-activated cell sorting (FACS). Pb*a* displayed different behavior if administered in its free form or as **DR2** conjugate. In particular, the uptake of free Pb*a* was significant already after 3 h in VCaP [MF (mean fluorescence) = 188.89] (Figure 4A), while a longer time (6 h) was required for **DR2** to reach a similar intracellular concentration [MF **DR2** in VCaP = 206] (Figure 4B). Pb*a* might passively translocate across cell membrane, while the more steric hindered **DR2** conjugate likely engages a different route to enter the cell. Furthermore, confocal microscopy analysis in Figure 4 (D and E), demonstrates that **DR2** exhibits a higher accumulation rate over time, as compared to Pb*a* alone. This behavior might be due to its affinity for AR expressed in VCaP cells.

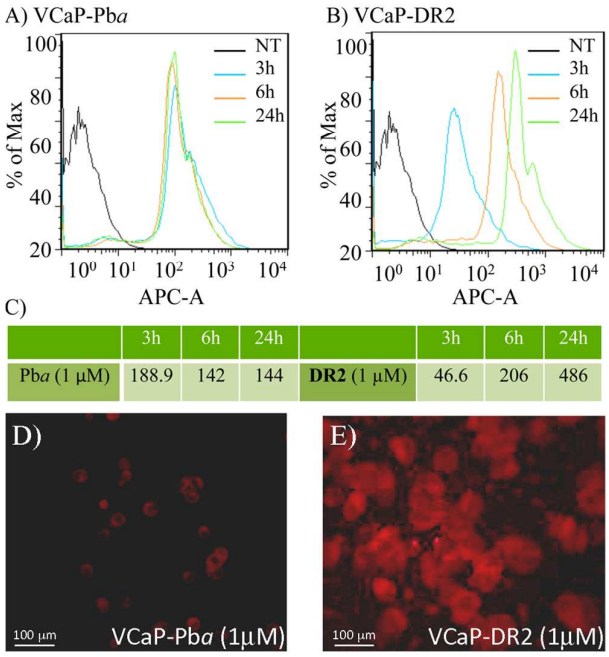

	3h	6h	24h		3h	6h	24h
Pb*a* (1 μM)	188.9	142	144	**DR2** (1 μM)	46.6	206	486

Figure 4. Uptake of Pb*a* and **DR2** on VCaP cells. **A) - B)** FACS analyses of VCaP cells treated with 1 μM of Pb*a* and **DR2**. **C**) Values of Mean of Fluorescence (MF) at different time of photosensitizer incubation. Fluorescence was detected after 3, 6 and 24 h from compound incubation. Data were collected from three different experiments **D) - E)** High magnification (40X) single plane confocal images representative of fluorescence emission collected by VCaP cells after 6 h of incubation with 1μM Pb*a* (**D**) and 1μM **DR2** (**E**). Bar is 100 μm.

***DR2** in vitro uptake and internalization studies in malignant PC cells.*

Prostate cancer-derived PC3 cells are highly metastatic and androgen-insensitive as they express low levels of the AR, thus representing a valuable *in vitro* model of castration-resistant PC.[30,31] In order to evaluate the ability of our conjugate to be internalized by these cells, we analyzed by FACS analysis the delivery/uptake of Pb*a* and **DR2** in PC3 cells. Data in Figure 5A show that as it occurs in VCaP cells (Figure 4A), the uptake of free Pb*a* in PC3 cells is significant already after 3 h (MF 302.88), while 6 h were required for the uptake of **DR2** (MF 170). Confocal microscopy images in Figure 5 (D and E) show that Pb*a* and **DR2** are both diffused in cytoplasm compartment after 6 h incubation. Interestingly, when comparing confocal microscopy images of **DR2** in VCaP and PC3 cells after 6 h of incubation, we observed that while in PC3 cells **DR2** is localized exclusively in the cytoplasm, in VCaP cells red fluorescence is intensively diffused also in the nucleus (cfr Figures 4E and 5E). This result might suggest that **DR2** translocates into the nucleus upon binding to the receptor, as also confirmed by the binding experiment performed with the radio-ligand assay (Figure 3). However, more studies are underway to verify the role of **DR2** after the binding to the androgen receptor in terms of gene transcription activity.

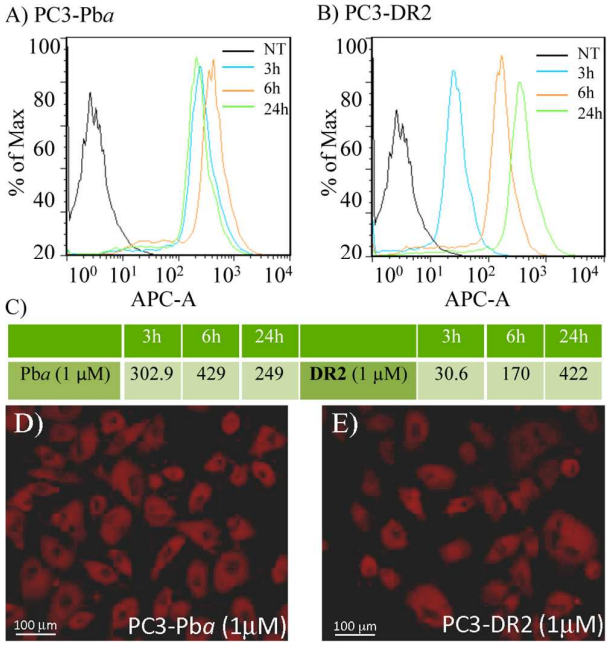

	3h	6h	24h		3h	6h	24h
Pb*a* (1 µM)	302.9	429	249	**DR2** (1 µM)	30.6	170	422

Figure 5. Uptake of Pb*a* and **DR2** on PC3 cells. **A) - C)** FACS analyses of PC3 cells treated with 1 µM of Pb*a* and **DR2**. **C**) Values of Mean of Fluorescence after different time of photosensitizer incubation. Fluorescence was detected after 3, 6 and 24 h from compound incubation. Data were collected from three independent experiments **D) - E)** High magnification (40X) single plane confocal images representative of fluorescence emission collected by PC3 cells after 6 h of incubation with 1µM Pb*a* (**D**) and 1µM **DR2** (**E**). Bar is 100 µm.

Despite **DR2** internalization seems to be slightly slower in PC3 cells as compared to VCaP cells (cfr. Figure 4C and 5C), **DR2** is persistently present after 24 h of incubation in PC3 cells (MF 422). In contrast, the amount of Pb*a* is significantly reduced (MF 249) at that incubation time (Figure 5C), likely because of its efflux. This behavior draw our attention to the emerging problem of PDT resistance,[32] and in particular to

Pb*a* as substrate for the ABCG2 pump efflux.[33–35] The ABCG2 gene encodes a membrane transporter belonging to the ATP-binding cassette (ABC) superfamily of membrane transporters, which being involved in the trafficking of a variety of biological molecules and drugs across the plasma membrane, also plays a role in multidrug resistance. To investigate more deeply this aspect and the possible beneficial role of conjugating the photosensitizer with specific targeting antenna, we performed an experiment with A549 human lung adenocarcinoma cells that express higher levels of ABCG2, as compared with PC3 cells (Figure 6A-B).

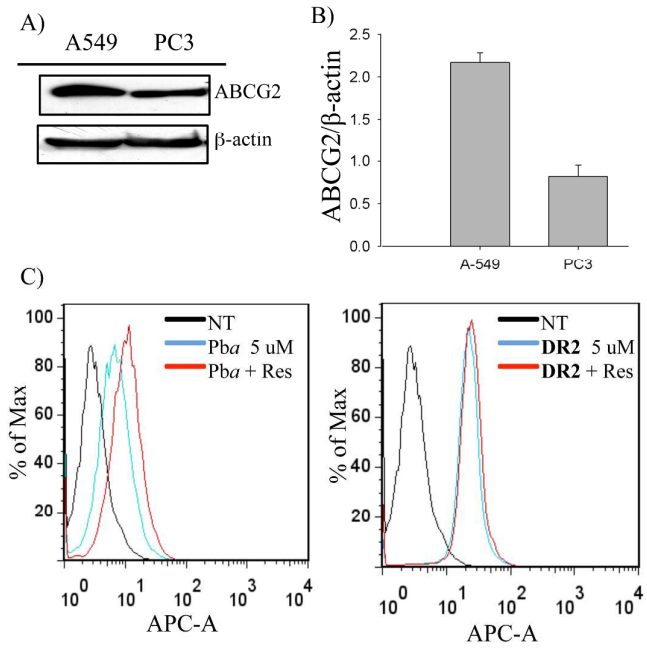

Figure 6. **A**) Western Blot of ABCG2 and β-actin protein levels in A549 and PC3 cell lines. **B**) The histograms report the values of the ABCG2 protein band intensity determined by densitometric analysis and normalized for β-actin. **C**) Functional assay for ABCG2 substrate. The A549 cells were incubated with 5 μM of Pb*a* or **DR2** for 30 min with or without 10 μM reserpine, washed, and then incubated for 60 min in PS-free media with (red line) or without (blu line) reserpine. Intracellular fluorescence was determined using a flow cytometer equipped with a 633 nm red diode laser. Representative results from two independent experiments are shown.

Robey and co-workers described a functional assay to evaluate if different photosensitizers are substrates for this efflux pump, using an ABCG2 inhibitor, e.g. reserpine.[34,36,37] Therefore, in order to determine whether **DR2** is a substrate for ABCG2 pump, we incubated A459 cells with 5μM of Pb*a* or **DR2** in the presence or absence 10 μM of reserpine for 30 min. Subsequently, the cells were washed and incubated for 1 h in a photosensitizer-free medium in the presence of reserpine. Graphs in Figure 6C report the fluorescence of Pb*a* (left) and **DR2** (right), alone (blue lines) or plus reserpine (red lines), respectively. Reserpine increases the accumulation of Pb*a* in the PC3 cells, while no shift of the fluorescence peak is observed by using **DR2**, thus suggesting that **DR2** is not a substrate for the efflux pump.

In sum, data in Figures 4, 5 and 6 show that **DR2** conjugate binds with high affinity AR and escapes the ABCG2 efflux pump in PC3 cells. These properties make **DR2** a promising candidate for PDT in PC, since it

is retained in PC cells expressing different levels of AR. In this latter setting, **DR2** consistently accumulates within PC cells, preventing the onset of PDT resistance.[32]

In vitro photodynamic activity

The *in vitro* photodynamic activity of **DR2** was investigated against LNCaP, VCaP and PC3 cells. Twenty-four h after light irradiation, cell proliferation was determined by resazurin assay using free Pb*a* as reference. Pb*a* presents a Q band absorption peak at 670 nm allowing irradiation with a red light, while the *o*-CF_3 nitrobenzene group (AR ligand moiety) should release NO upon selective irradiation at 400 nm. Therefore, in order to stimulate both compounds, cells were initially irradiated with a white halogen light covering the entire visible spectrum.

According to the results of the uptake experiments, cells were incubated in the dark with increasing concentrations of Pb*a* and **DR2** for 6 h and subsequently irradiated with a metal white halogen lamp for 30 min (7 J/cm^2). Data shown in Figure 7 (A-C) account for a higher photo-toxicity of **DR2** in all cell lines as compared to Pb*a* alone. Remarkably, the IC_{50} values (defined as the compound concentration to inhibit 50% of the cells) of **DR2** were lower than Pb*a* in all cell lines (Table 1), when using white light. This might be due to the longer retention of **DR2** inside the cells and to the ability of the NO-donor moiety to induce the release of NO species that are synergistic to $^1O_2$ generated by Pb*a*. Importantly, no dark toxicity was observed for the conjugate 24 h after treatment (Figure S2).

In order to evaluate the contribution of NO to the overall toxicity of the new conjugate, we performed a second set of metabolic assays using a halogen lamp equipped with a red filter, with the aim to excite only Pb*a*. Results on PC3, LNCaP and VCaP cells are reported in Figure 7 (D-F) and Table 1, confirming that no difference occurs in the photo-toxic behavior of the two compounds when irradiated with red light, thereby supporting the additive action of the NO released only when white lamp is used as light source.

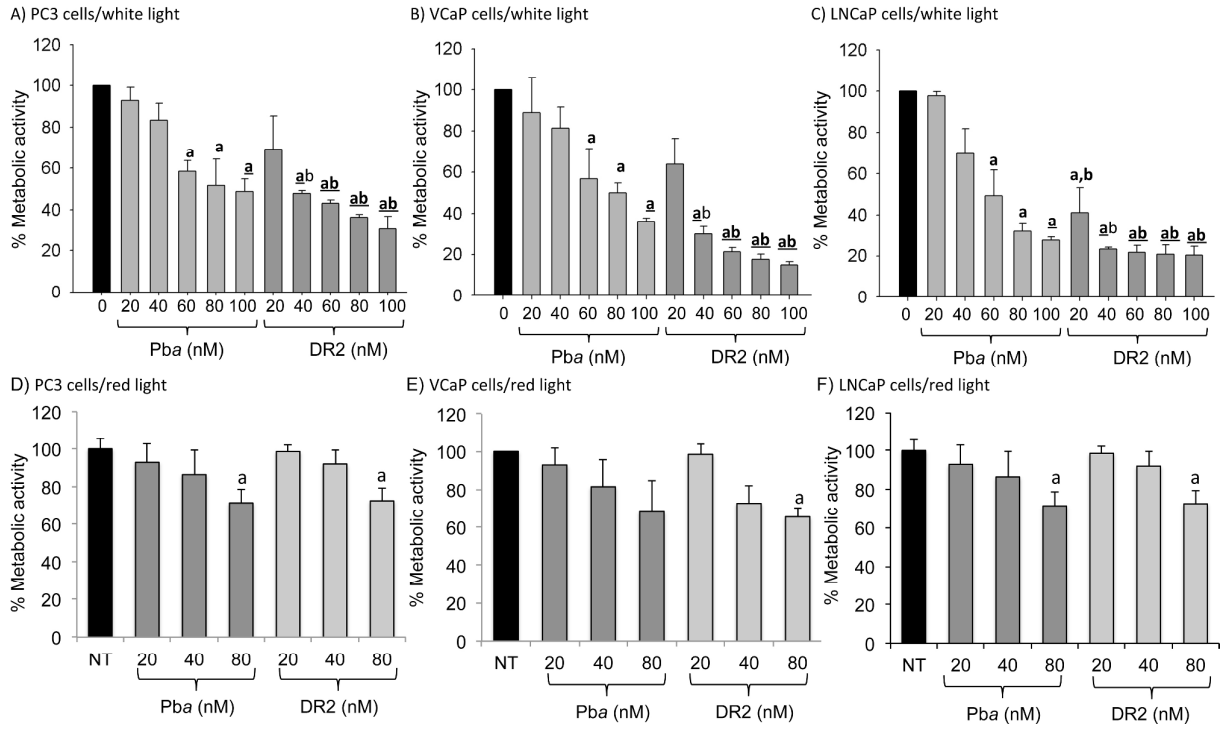

Figure 7. %Metabolic activity of PC3, VCaP and LNCaP cells treated with increasing amounts of Pb*a* and **DR2**. After 6 h incubation in the dark the cells were irradiated **A-C**) with a white halogen lamp (fluence 7.2 J/cm^2) and **D-F**) with the same lamp equipped with a red filter (fluence 0.84 J/cm^2). A resazurin assay was carried out 24 h after irradiation. Data represent mean values ± SD of three independent experiments. T-Test analysis of different treatments (Pb*a* and DR2) *vs* NT **a**: p<0.05; **a**: p<0.01**;** DR2 vs Pba: **b** p<0.05; **b:** p<0.01.

Table 1. IC_{50} values of Pb*a* and **DR2** upon white and red light irradiation on a panel of prostate cancer cell lines[a]

	IC_{50}[nM]					
Compound	**VCaP**[b,c]		**LNCaP**[b,c]		**PC3**[b,c]	
	white light	**red light**	**white light**	**red light**	**white light**	**red light**
Pb*a*	78.9±0.96	94±3.2	60.1±2.1	65±5	82.1±1.9	95±6
DR2	25.3±1.10	96±5.0	12.0±1.4	70±6	35.1±2.8	98±5

[a]Six hours after incubation in the dark with the compounds, cells were irradiated whit a metal white halogen lamp (alone or equipped with a red filter) for 30 min. [b]The reported values are the IC_{50} expressed in nanomolar. [c]$P < 0.05$ (t-test) **DR2** vs Pb*a*. Data represent mean values ± SD of three independent experiments.

In parallel a Griess test was performed to evaluate the nitrite production. After 24 h incubation at 37°C, the cells were treated with different concentrations of Pb*a* and **DR2** and irradiated with white or red light. After 1 h from irradiation the cell supernatants were collected and NO production was evaluated by addition of the Griess reagent. Nitrite concentration was determined by measuring the absorbance at 540 nm with respect to a standard curve of $NaNO_2$ diluted in culture medium.

Data reported in Figure 8 successfully account for a higher nitrite production by **DR2,** as compared to Pb*a* under white light irradiation. This effect is particularly evident in VCaP cells (Figure 8A). The extent of NO_2 production induced by red light is almost negligible (Figure 8B), thus confirming the effective production of NO radicals induced by the AR ligand present on the **DR2** backbone.

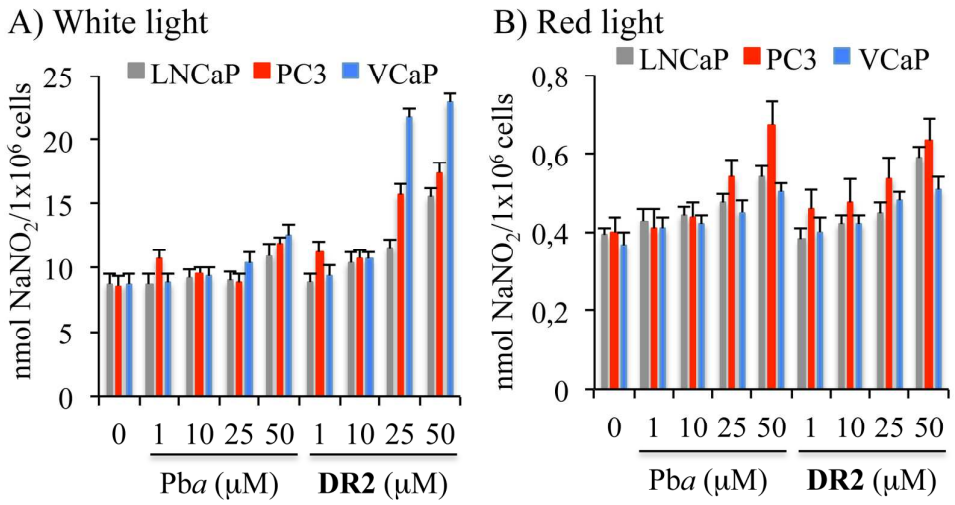

Figure 8. Nitric oxide detection by Griess test. Effects of different amounts (0-50 μM) of Pb*a* and **DR2** on nitric oxide production in PC cells after **A)** white light irradiation and **B)** red light irradiation. Nitrite concentrations were determined by comparing the absorbance values for the test samples to a standard curve generated by serial dilution of 100 mmol/L sodium nitrite. Results of NO production are expressed as nmol $NO_2^-/10^6$ cells and are collected from two different experiments.

In conclusion, the reported data indicate that **DR2** is a novel and promising photosensitizer for the multi-modal treatment of prostate cancer. Cell death increase is observed in all considered cell lines. This effect is likely associated with the synergistic/additive action of the ROS generated by the photosensitizer moiety (Pb*a*) and the NO released upon irradiation of the AR ligand moiety with white light. Moreover, **DR2** exhibits a constant and time-dependent fluorescence increase even after 24 h of incubation in both VCaP and PC3 cells. This behavior might be due to the concomitant affinity of the conjugate for the AR that might favor its internalization and accumulation into tumor cells, and to the ability of **DR2** to escape the ABCG2 efflux pump mechanism which is responsible for Pb*a* to be excreted from the cells. This result is particularly important if considering that PC3 cells lack the AR and are representative of an advanced stage of the disease.

DR2 displays very promising features of selectivity and controlled phototoxicity in a variety of PC cell lines, while being totally non-toxic in the dark. Overall, these characteristics make **DR2** a promising candidate for further investigations in PC *in vivo* models.

Experimental Procedures

Materials chemistry: All solvents and reagents were used as obtained from commercial sources unless otherwise indicated. Solvents and reagents were obtained from Sigma-Aldrich (Schnelldorf, DE). Pb*a* was purchased from Frontier Scientific (Catalog # Pha-592) and used without further purification.

Materials biology: unlabeled R1881, bicalutamide, reserpine, PBS-0.01% Tween, Griess reagent [1% sulphanilamine in 30% acetic acid with 0.1% *N*-(naphthyl)ethylenediamine dihydrochloride in 60% acetic acid] and resazurin assay were obtained from Sigma–Aldrich, Milan, Italy and enzalutamide from Selleckchem. PC3 and VCaP cells were purchased from Experimental Zooprophylactic Institute of Lombardia and Emilia Romagna. Prostate cancer-derived fast-growing LNCaP cells were from ATCC (U.S.A.). A549 cells were obtained by Professor G. Tell (Department of Medical and Biological Sciences, University of Udine, Italy). Dulbecco's Modified Eagle Media (DMEM), Fetal Bovine Serum (FBS), Insulin, antibiotics (Penicillin/Streptomycin), RPMI1640 and Pen/Strepto, were purchased from Gibco. Non-targeting siRNAs, containing a scrambled sequence, rabbit polyclonal anti-AR (N-20) or anti ABCG2 (B-25:sc-130933) antibodies were purchased from Santa-Cruz Biotechnologies. Mouse monoclonal antitubulin antibody was from Sigma-Aldrich. Lipofectamine^{TM} 2000 was from Invitrogen. [^{3}H]-R1881 (98 Ci/mmole) was purchased by Perkin Elmer. Mouse monoclonal anti β-actin (Ab-1, CP01), anti-rabbit IgG and anti-mouse IgM were obtained from Calbiochem. Super Signal®West PICO and Super Signal®West FEMTO were from ThermoFisher Scientific Pierce, Rockford, USA.

Methods chemistry: All reactions were performed under nitrogen atmosphere unless otherwise noted. Flash chromatography was performed on Teledyne Isco CombiFlash® Rf 200 using RediSep® Normal-phase Silica Flash Columns (230–400 mesh). The reactions were monitored by TLC using silica gel 60 F254 with detection by charring with $KMnO_4$. UV spectra were registered with a Lambda 20 Perkin Elmer spectrophotometer. NMR spectra were recorded in $CDCl_3$, $(CD_3)_2CO$ or CD_3OD solutions at 25 °C on a Varian Mercury spectrometer operating at 400 MHz (1H) and 100.5 MHz (13C). When present, the water signal in the ^{1}H NMR spectra was suppressed using post-elaboration solvent suppression sequence.

^{1}H Chemical shifts values (δ) are referenced to the residual non-deuterated components of the NMR solvents (δ = 7.26 ppm for $CHCl_3$ and δ = 3.31 ppm for CHD_2OD, etc.). The 13C chemical shifts (δ) are referenced to $CDCl_3$ (central peak, δ = 77.0 ppm), CD_3OD (δ = 49.0 ppm), etc. as the internal standard. The IR spectra were registered with a Perkin Elmer Spectrum BX FT-IR System. For accurate mass measurements, the compounds were analyzed in positive ion mode by Agilent 6520 HPLC-Chip Q/TOF-MS (nanospray) using a quadrupole, a hexapole and a time-of-flight unit to produce the spectra. The capillary source voltage was set to 1700 V; the gas temperature and drying gas were kept at 350 °C and 5 L min−1, respectively. The MS analyzer was calibrated externally with the ESI-L low concentration tuning mix from m/z 118 to 2700 to yield an accuracy below 5 ppm. Accurate mass data was collected by directly infusing samples in 40/60 H2O/ACN 0.1% TFA into the system at a flow-rate of 0.4 μL min−1. FEP tubing, 1/16″ °- 1.0 mm ID and PTFE tubing, 1/16″ °- 1.0 mm ID were purchased from VICI Jour.

Chemistry

Acid 1. Methyl ester (**S2**) (1 eq.) was than dissolved in methanol (10 mL/mmol) and few drops of THF. NaOH (1N) (1 eq.) was then added to the solution, which was than stirred for 24 h at room temperature. A white precipitate formed that was filtered off and dry under vacuum affording acid (**1**) as pure compound in 80%. ^{1}H NMR (400 MHz, CD_3OD) δ 9.03 (bs, 1H), 8.37 (d, J = 8.7 Hz, 1H), 8.26 (d, J = 8.2 Hz, 1H), 8.04 (d, J = 8.9 Hz, 1H), 7.26 (d, J = 1.9 Hz, 1H), 7.19 (d, J = 9.1 Hz, 1H), 4.62 (bs, 1H), 4.39 (bs, 1H), 4.01 (d, J = 13.5 Hz, 1H), 3.73 – 3.54 (m, 2H), 3.55 (d, J = 12.0 Hz, 1H), 1.34 (d, J = 6.0 Hz, 3H, CH_3), 1.25 (d, J = 6.4 Hz, 3H, CH_3). ^{13}C NMR (100 MHz, CD_3OD) δ 171.84, 155.26, 153.35, 142.27, 137.69, 137.01, 136.74, 130.48, 128.64, 126.58, 124.14, 121.43, 115.25, 111.70, 60.38, 49.72, 45.29, 43.12, 14.98, 12.25. HRMS (m/z) calcd for $C_{20}H_{20}F_3N_5O_5$ [M]+, 468.1417; found, 468.1420.

Activated acid 2. N-hydroxysuccinimide (1 equiv) and DCC (1 equiv) were subsequently added to a solution of the acid (**1**) (1 equiv) in 1,4-dioxane (14 mL/mmol of **1**). The reaction mixture was stirred at room temperature for 5 h and then diluted with THF. The obtained solution was absorbed on SiO_2 and evaporated under vacuum. The resulting solid was purified by silica gel flash chromatography (CH_2Cl_2/Et_2OAc/*c*Hex = 1/2/2) affording the desired compound in 70% yield. ^{1}H NMR (400 MHz, CD_3OD) δ 8.87 (bs, 1H), 8.24 – 8.12 (m, 2H), 8.04 (d, J = 9.2 Hz, 1H), 7.26 (d, J = 2.3 Hz, 1H), 7.18 (dd, J^1 = 9.4, J^2 = 2.8 Hz, 1H), 4.62 – 4.56 (m, 1H), 4.40 – 4.32 (m, 1H), 4.25 – 4.17 (m, 1H), 3.99 – 3.91 (m, 1H), 3.73 – 3.65 (m, 2H), 2.91 (s, 4H, 2 CH_2), 1.33 (d, J = 6.7 Hz, 3H, CH_3), 1.23 (d, J = 6.6 Hz, 3H, CH_3). ^{13}C NMR (100 MHz, CD_3OD) δ 171.70, 156.67, 154.52, 143.50, 142.58, 137.38, 136.74, 130.48, 128.64, 126.58, 124.14, 116.34, 112.78, 49.72, 48.47, 48.04, 45.29, 43.12, 26.7, 16.10, 13.46. HRMS (m/z) calcd for $C_{24}H_{23}F_3N_6O_7$ [M]+, 565.1580; found, 565.1585.

Compound 3. To a solution of *tert*-butyl (2-(2-(2-aminoethoxy)ethoxy)ethyl)carbamate[32] (1 eq.) in dry THF (3.2 mL/mmol), pyridine (1.4 mL/mmol) was added drop wise followed by succinimidyl derivative (**2**) (1 eq.). The reaction mixture was then stirred at room temperature for 24 h (complete disappearance of the starting material). The mixture was then diluted with EtOAc and the organic layer was washed several times with distilled water. The collected organic phase was then dried over Na_2SO_4, filtered and evaporated under reduced pressure. The crude material was successively treated with CF_3COOH (28 mL/mmol of starting acid) and stirred at room temperature for 3 h. The reaction mixture was subsequently diluted with distilled water and basified (pH = 10) with $NaHCO_3$. The organic phase was then extracted with EtOAc and dried over anhydrous Na_2SO_4, filtered and concentrated under reduced pressure to afford (**3**) as pure compound in 70% yield. ^{1}H NMR (400 MHz, CD_3OD) δ 8.73 (bs, 1H), 8.05 (d, J = 9.6 Hz, 3H), 7.27 (d, J = 2.8 Hz, 1H), 7.21-7.11 (m, 1H), 4.63-4.57 (m, 1H), 4.41 – 4.32 (m, 1H), 4.02 – 3.92 (m, 2H), 3.69-3.54 (m, 6H), 3.55 – 3.39 (m, 2H), 2.94 – 2.75 (m, 1H), 1.33 (d, J = 6.6 Hz, 3H, CH_3), 1.24 (d, J = 6.7 Hz, 3H, CH_3). ^{13}C NMR (101 MHz, CD_3OD) δ 165.54, 156.08, 153.38, 150.16, 143.58, 140.53, 134.29, 132.05, 131.32, 128.60, 127.39, 122.09, 115.21, 75.95, 70.18, 70.15, 69.46, 51.80, 49.78, 45.33, 43.06, 40.10, 39.05, 25.57, 24.88, 14.93, 12.27. HRMS (m/z) calcd for $C_{26}H_{33}F_3N_6O_7$ [M]+, 599.2363; found, 599.2370.

Conjugate DR2. Compounds (**4**) (see Supporting information for detailed synthesis) (1 eq.) and (**3**) (1.2 eq.) were placed in a two-necked round bottomed flask under nitrogen and in the dark. Then, THF (40 mL/mmol) was added followed by pyridine drop wise (16 mL/mmol). The reaction mixture was stirred at room temperature for 24 h, monitoring the disappearance of the starting material by TLC. The reaction mixture was then diluted with EtOAc and washed several times with distilled water. The collected organic phases were then dried over Na_2SO_4, filtered and concentrated under reduced pressure. The crude material was then purified by silica gel flash column chromatography (CH_2Cl_2/MeOH = 14/1) affording **DR2** in 98% yield. ^{1}H NMR (400 MHz, $CDCl_3$) δ 9.41 (d, *J* = 11.7 Hz, 1H), 9.31 (d, *J* = 6.4 Hz, 1H), 8.61 (bs, 1H), 8.51 (bs, 1H), 8.42 (bs, 1H), 8.19-8.15 (m, 1H), 8.11 – 7.90 (m, 3H), 7.68 (dd, J_1 = 10.4 Hz; J_2 = 3.0 Hz, 1H), 7.29 (dd, J_1 = 7.6 Hz; J_2 = 5.0 Hz, 1H), 6.32 – 6.16 (m, 3H), 4.49-4.37 (m, 2H), 4.23-4.15 (m, 3H), 3.87 (d, *J* = 9.0 Hz, 3H), 3.75-61 (m, 7H), 3.52 – 3.39 (m, 7H), 3.36 (d, *J* = 3.6 Hz, 6H), 3.20 (d, *J* = 5.2 Hz, 6H), 2.50-2.38 (m, 4H), 1.83 (d, *J* = 7.6 Hz, 3H), 1.75 (d, *J* = 7.3 Hz, 3H), 1.33 (d, *J* = 6.8 Hz, 3H), 1.23 (d, *J* = 6.8 Hz, 3H). ^{13}C NMR (101 MHz, $CDCl_3$) δ 189.80, 173.12, 172.44, 170.32, 164.51, 157.09, 154.88, 152.71, 149.98, 145.66, 144.05, 142.59, 139.70, 139.19, 138.03, 137.06, 136.68, 132.45, 129.04, 127.52, 126.66, 126.26, 123.84, 123.38, 122.77, 121.12, 114.39, 111.84, 104.68, 93.77, 93.56, 70.13, 69.79, 65.18, 53.37, 51.61, 50.55, 49.34, 46.84, 45.56, 43.20, 39.13, 34.16, 33.38, 30.56, 29.92, 25.81, 25.16, 23.33, 19.62, 17.54, 16.06, 13.10, 12.30, 11.43. HRMS (m/z) calcd for $C_{61}H_{68}F_3N_{11}O_{10}$ [iM]+, 1172.5103; found, 1172.5109.

Cell culture experiments

Cell culture.

PC3 and LNCaP cells were cultured in RPMI 1640 medium, while VCaP and A549 cells in DMEM. Both media contained 10% FBS, antibiotics (penicillin 100 U/ml, streptomycin 100 μg/ml) and glutamine 2 mM. Cells were maintained in a humidified atmosphere with 5% CO_2 air at 37 °C. Unless otherwise stated, experiments were performed using cells at the exponential growth phase.

siRNA AR experiments and AR ligand binding displacement studies.

For AR binding experiment LNCaP cells were cultured in RPMI 1640 supplemented with 10% fetal calf serum and made quiescent as reported.[27] After reaching sub-confluence, growing LNCaP cells were used for AR siRNA experiments, using a pool of 4 target-specific 20-25 non-targeting or AR siRNAs, as reported.[38] siRNAs were transfected using Lipofectamine™ 2000. After transfection, the cells were kept in phenol red-free RPMI 1640 medium containing 5% charcoal-stripped calf serum and Pen/Strepto for 24 hrs. Transfected cells were then used for ligand binding studies or WB analysis. For AR ligand binding studies, untransfected or transfected LNCaP cells were incubated at 37°C for 4h with 10 nM of [^{3}H] R1881 to the medium, in the absence or presence of the indicated excess of radio-inert compounds (R1881, bicalutamide, enzalutamide or DR2), as previously described.[39] Cells were then washed three times with ice-cold PBS and collected by gently scraping in the cold room using 600 μL of ice-cold PBS containing 0.05% EDTA (w/v). The number of cells in an aliquot of 100 μl was counted. Aliquots (400 μl) of cell suspension were used in duplicate to extract the intracellular radioactivity in 1000 μl ice-cold ethanol (100%) for 2 h. After 24 h at 37°C, the

radioactivity was counted in a liquid scintillation counter. Non-specific binding of [^{3}H]-R1881 was always determined in separate wells by adding 1 μM of unlabeled R1881 to the incubation medium, as a control. The Western blot analysis was done using cell lysates (at 2 mg/ml protein concentration) as described.[24] AR was detected using the rabbit polyclonal anti-AR antibodies (N-20; Santa Cruz). The mouse monoclonal anti-tubulin antibody (Sigma) was used to detect tubulin. Immune-reactive proteins were revealed using the ECL detection system (GE Healthcare).

Fluorimetric determination of cellular uptake.

VCaP, LNCaP and PC3 cells were seeded in a 6-well plate at a cell density of 6×10^5cells/well. The day after, the cells were treated with Pb*a* and **DR2** at concentration of 1 μM. At different time of incubation in the dark (3-6-24 h), the cells were harvested, washed twice, resuspended in 0.5 mL of PBS and analyzed by a FACSARIA 3 (Becton Dickinson, San Jose, USA) equipped with a 633 nm laser. A minimum of 10,000 cells for sample was acquired in list mode and analyzed using FLOWJO software. The signal was detected by APC-A in log scale.

Confocal microscopy studies

VCaP and PC3 were seeded on 19 mm coverslips coated with FBS, evaporated overnight, placed into 12 multi-well plate at the concentration of $5x10^3$ per sample, thus allowing to reach the best cells confluence at 24 h, and to perform imaging experiments. Pba and **DR2** [1 μ□] were then added to the cells medium from a stock solution (1mL) and then samples were kept in the incubator covered from the light. After 4 h of incubation, all the samples have been washed three times for 1 min with PBS before performing confocal experiments. Optical imaging has been performed with a Nikon TE 2000 inverted confocal microscope equipped with 40X objective and Hamamatsu CCD camera. Coverslips were then mounted by means of a custom made chamber onto Nikon TE2000 inverted microscope and fluorescence images were collected at 543 nm He Ne laser as excitation source. Images reported are representative of 2 different experiments, performed in triplicate.

Expression of ABCG2 by western blotting.

For this experiment we have compared the protein level of ABCG2 in A549 lung carcinoma cells and in PC3 cells. The extracted proteins (40 μg) were subjected to electrophoresis on 12% SDS–PAGE and transferred to a nitrocellulose membrane 70 V for 2 h. The filter was blocked for 1 h with PBS-0.01% Tween containing 5% dry non-fat-milk, and then incubated, at 4 °C overnight, with the primary antibody, rabbit polyclonal ABCG2 diluted 1:100. The expression of β-actin, used as an internal control, was detected with a mouse monoclonal anti β-actin (Ab-1, CP01) diluted 1:10,000. The filters were incubated for 1 h with the secondary antibodies with either anti-rabbit IgG diluted 1:4000 or anti-mouse IgM, diluted 1:5000. Each secondary antibody was coupled to horseradish peroxidase (HPR). For the detection of the proteins, we used ECL (enhanced chemiluminescence) reagents (Super Signal®West PICO, and Super Signal®West FEMTO). The

exposure length depended on the antibodies used and was usually between 30 s and 5 min. The protein levels were quantified by Image Quant TL Version 2003 software (Amersham).

Flow cytometry Pba and DR2 uptakes after ABCG2 inhibitor treatment.

A549 cells were seeded at the density of $6x10^5$ cells/well. The day after, cells were incubated (30 min in the dark) in complete medium with the desired photosensitizer (5 μM Pb*a* or **DR2**) with or without 10 μM of ABCG2 inhibitor, reserpine (Sigma-Aldrich, Milan, Italy) an ABCG2 inhibitor. After this time, the cells were incubated in photosensitizer-free fresh medium, with or without 10 μM reserpine for 1 h. The cells were harvested, washed twice and resuspended in PBS. The photosensitizer uptake was measured by FACSARIA 3 (Becton Dickinson, San Jose, USA) equipped with a 633 nm laser. A minimum of 10,000 cells for sample was acquired in list mode and analyzed using FLOWJO software. The signal was detected by APC-A in log scale.

Photodynamic treatment.

Pb*a* and **DR2** were dissolved in dimethylsulfoxide (DMSO) and conserved in aliquots of 0.5 mM at -80°C. Their stability in solution was checked by measuring their UVvis spectrum at weekly intervals. Cells were incubated with different concentration of the compounds in the dark and then irradiated whit a metal white halogen lamp for 30 min (7 J/cm^2) or with red filter for 7 min (0.84 J/cm^2) depending on the experimental conditions. Fluency for red light was assessed on the basis of the IC_{50} of Pb*a* with white light.

Cell metabolic assay.

PC cells were seeded in a 96-well plate at a density of $5x10^3$ cells/well. The following day, Pb*a* and **DR2** were added at different concentrations and incubated for 6h in the dark and then light irradiated. 24 h after irradiation the metabolic activity was determined by the resazurin assay following the manufacturer's instructions (Sigma–Aldrich, Milan, Italy). The fluorescence was measured with a spectrofluorimeter (EnSpireTM 2300 Multilabel reader, PerchinElmer, Finland). The data are presented as the percentage of metabolic activity compared to untreated cells. The data are the average of at least three independent experiments. The protocol for PDT is reported in the figure captions.

Nitric oxide detection by Griess test.

PC cells were seeded in a 96-well plate at a density of 10^4cells/well. After 24-h incubation at 37 C, the cells were treated with different concentrations of Pb*a* and **DR2** in DMEM without phenol red. After 24 h, cells were irradiated with white or red light and after 1 h equal volumes of culture supernatants were collected and mixed. Cell supernatants were collected and mixed with Griess reagent (Sigma-Aldrich). After incubation at room temperature for 15 minutes, the absorbance was measured at 540 nm with EL808 Ultra Microplatet Reader (BIO-TEK Instruments, Inc, Vermont USA). Nitrite concentrations were determined by comparing the absorbance values for the test samples to a standard curve generated by serial dilution of 100 mmol/L sodium nitrite. Results of NO production are expressed as nmol $NO_2^-/10^6$ cells.

Acknowledgments

The work done by Prof. Gabriella Castoria and Dr. Marzia Di Donato was supported by grants from the Italian Ministry of University and Scientific Research (P.R.I.N. 2010NFEB9L_002). M.D.D is a recipient fellowship of a PRIN Grant (2010NFEB9L_002).

"Supporting Information Available: experimental procedures, spectroscopic data and copies of $^{1}H/^{13}C$ NMR of new compounds; additional figures and tables on biological experiments. This material is available free of charge via the Internet at http://pubs.acs.org."

Abbreviations

ABC, ATP-binding cassette; ABCG2, ATP-binding cassette sub-family G member 2; ADP, androgen receptor therapy; AR, androgen receptor; CF_3, trifluoromethyl; CRPC, castration-resistant prostate cancer; DCC, *N,N*'-Dicyclohexylcarbodiimide; GPRC6A, *G protein*-coupled receptor, class C, group 6, member A; HRMS, High Resolution Mass Spectroscopy; MF, mean of fluorescence; NMR, Nuclear Magnetic Resonance; NO, nitric oxide; PC, prostate cancer; PDT, photodynamic therapy; PS, photosensitizer; ROS, reactive oxygen species; siRNA, small interference RNA; THF, tetrahydrofuran.

References

(1) Jemal, A., Siegel, R., Ward, E., Hao, Y., Xu, J., and Thun, M. J. (2009) Cancer statistics, 2009. *CA. Cancer J. Clin. 59*, 225–249.

(2) Oudard, S. (2013) Progress in emerging therapies for advanced prostate cancer. *Cancer Treat. Rev. 39*, 275-289.

(3) Clegg, N. J., Wongvipat, J., Joseph, J. D., Tran, C., Ouk, S., Dilhas, A., Chen, Y., Grillot, K., Bischoff, E. D., Cai, L., et al. (2012) ARN-509: a novel antiandrogen for prostate cancer treatment. *Cancer Res. 72*, 1494–1503.

(4) Berthold, D. R., Sternberg, C. N., and Tannock, I. F. (2005) Management of advanced prostate cancer after first-line chemotherapy. *J. Clin. Oncol. 23*, 8247–8252.

(5) Tannock, I. F., De Wit, R., Berry, W. R., Horti, J., Pluzanska, A., Chi, K. N., Oudard, S., Théodore, C., James, N. D., Turesson, I., et al. (2004) Docetaxel plus prednisone or mitoxantrone plus prednisone for advanced prostate cancer. *N. Engl. J. Med. 351*, 1502–1512.

(6) Beltran, H., Beer, T. M., Carducci, M. A., De Bono, J., Gleave, M., Hussain, M., Kelly, W. K., Saad, F., Sternberg, C., Tagawa, S. T., et al. (2011) New therapies for castration-resistant prostate cancer: efficacy and safety. *Eur. Urol. 60*, 279–290.

(7) Mohler, M. L., Coss, C. C., Duke, C. B., Patil, S. A., Miller, D. D., and Dalton, J. T. (2012) Androgen receptor antagonists: a patent review (2008-2011). *Expert Opin. Ther. Pat. 22*, 541–565.

(8) Balbas, M. D., Evans, M. J., Hosfield, D. J., Wongvipat, J., Arora, V. K., Watson, P. A., Chen, Y., Greene, G. L., Shen, Y., and Sawyers, C. L. (2013) Overcoming mutation-based resistance to antiandrogens with rational drug design. *Elife 2*, e00499.

(9) Nique, F., Hebbe, S., Peixoto, C., Annoot, D., Lefrançois, J.-M., Duval, E., Michoux, L., Triballeau, N., Lemoullec, J.-M., Mollat, P., et al. (2012) Discovery of diarylhydantoins as new selective androgen receptor modulators. *J. Med. Chem. 55*, 8225–8235.

(10) Koupparis, A., and Gleave, M. E. (2010) Multimodal approaches to high-risk prostate cancer. *Curr. Oncol. 17*, Supp. 2, S32-S37.

(11) Dolmans, D. E. J. G. J., Fukumura, D., and Jain, R. K. (2003) Photodynamic therapy for cancer. *Nat. Rev. Cancer 3*, 380–3877.

(12) Azzouzi, A.-R., Barret, E., Moore, C. M., Villers, A., Allen, C., Scherz, A., Muir, G., De Wildt, M., Barber, N. J., Lebdai, S., and Emberton, M. (2013) TOOKAD(®) Soluble vascular-targeted photodynamic (VTP) therapy: determination of optimal treatment conditions and assessment of effects in patients with localised prostate cancer. *BJU Int. 112*, 766–774.

(13) Agostinis, P., Berg, K., Cengel, K. A., Foster, T. H., Girotti, A. W., Gollnick, S. O., Hahn, S. M., Hamblin, M. R., Juzeniene, A., Kessel, D., Korbelik, M., Moan, J., Mroz, P., Nowis, D., Piette, J., Wilson, B. C., and Golab, J. (2011) Photodynamic therapy of cancer: an update. *CA. Cancer J. Clin. 61*, 250–281.

(14) Yoon, I., Li, J. Z., and Shim, Y. K. (2013) Advance in photosensitizers and light delivery for photodynamic therapy. *Clin. Endosc. 46*, 7–23.

(15) Kinoyama, I., Taniguchi, N., Toyoshima, A., Nozawa, E., Kamikubo, T., Imamura, M., Matsuhisa, A., Samizu, K., Kawanimani, E., Niimi, T., et al. (2006) (+)-(2R,5S)-4-[4-cyano-3-(trifluoromethyl)phenyl]-2,5-dimethyl-N-[6-(trifluoromethyl)pyridin-3- yl]piperazine-1-carboxamide (YM580) as an orally potent and peripherally selective nonsteroidal androgen receptor antagonist. *J. Med. Chem. 49*, 716–726.

(16) Dreaden, E. C., Gryder, B. E., Austin, L. A., Tene Defo, B. A., Hayden, S. C., Pi, M., Quarles, L. D., Oyelere, A. K., and El-Sayed, M. A. (2012) Antiandrogen gold nanoparticles dual-target and overcome treatment resistance in hormone-insensitive prostate cancer cells. *Bioconjug. Chem. 23*, 1507–1512.

(17) Gryder, B. E., Akbashev, M. J., Rood, M. K., Raftery, E. D., Meyers, W. M., Dillard, P., Khan, S., and Oyelere, A. K. (2013) Selectively targeting prostate cancer with antiandrogen equipped histone deacetylase inhibitors. *ACS Chem. Biol. 8*, 2550–2560.

(18) Carpenter, A. W., and Schoenfisch, M. H. (2012) Nitric oxide release: part II. Therapeutic applications. *Chem. Soc. Rev. 41*, 3742–3752.

(19) Jenkins, C. D., Charles, I. G., Thomsen, L. L., Moss, D. W., Holmes, L. S., Baylis, S. A., Rhodes, P., Westmore, K., Emson, P. C., and Moncada, S. (1995) Role of nitric oxide in tumor growth. *Proc. Nat. acad. Sci. USA 92*, 4392–4396.

(20) Gupta, S., Ahmad, N., and Mukhtar, H. (1998) Involvement of nitric oxide during phthalocyanine (Pc4) photodynamic therapy-mediated apoptosis. *Cancer Res. 58*, 1785–1788.

(21) Korbelik, M., Parkins, C. S., Shibuya, H., Cecic, I., Stratford, M. R., and Chaplin, D. J. (2000) Nitric oxide production by tumour tissue: impact on the response to photodynamic therapy. *Br. J. Cancer 82*, 1835–1843.

(22) Rapozzi, V., Della Pietra, E., Zorzet, S., Zacchigna, M., Bonavida, B., and Xodo, L. E. (2013) Nitric oxide-mediated activity in anti-cancer photodynamic therapy. *Nitric Oxide - Biol. Chem. 30*, 26–35.

(23) Carneiro, Z. A., De Moraes, J. C. B., Rodrigues, F. P., De Lima, R. G., Curti, C., Da Rocha, Z. N., Paulo, M., Bendhack, L. M., Tedesco, A. C., Formiga, A. L. B., and Da Silva, R. S. (2011) Photocytotoxic activity of a nitrosyl phthalocyanine ruthenium complex - A system capable of producing nitric oxide and singlet oxygen. *J. Inorg. Biochem. 105*, 1035–1043.

(24) Kim, J., Saravanakumar, G., Choi, H. W., Park, D., and Kim, W. J. (2014) A platform for nitric oxide delivery. *J. Mater. Chem. B 2*, 341-356.

(25) Sortino, S. (2010) Light-controlled nitric oxide delivering molecular assemblies. *Chem. Soc. Rev. 39*, 2903–2913.

(26) Nobuaki, T., Isao, K., Takashi, K., Akira, T., Kiyohiro, S., Eiji, K., Masakazu, I., Hiroyuki, M., Akira, M., Masaaki, H., et al. (2004) Cyanophenyl derivative Patent Number WO/2000/017163.

(27) Migliaccio, A., Castoria, G., Di Domenico, M., De Falco, A., Bilancio, A., Lombardi, M., Barone, M. V, Ametrano, D., Zannini, M. S., Abbondanza, C., et al. (2000) Steroid-induced androgen receptor-oestradiol receptor beta-Src complex triggers prostate cancer cell proliferation. *EMBO J. 19*, 5406–5417.

(28) Castoria, G., Giovannelli, P., Di Donato, M., Ciociola, A., Hayashi, R., Bernal, F., Appella, E., Auricchio, F., and Migliaccio, A. (2014) Role of non-genomic androgen signalling in suppressing proliferation of fibroblasts and fibrosarcoma cells. *Cell Death Dis. 5*, e1548.

(29) Tomlins, S. A., Rhodes, D. R., Perner, S., Dhanasekaran, S. M., Mehra, R., Sun, X.-W., Varambally, S., Cao, X., Tchinda, J., Kuefer, R., et al. (2005) Recurrent fusion of TMPRSS2 and ETS transcription factor genes in prostate cancer. *Science 310*, 644–648.

(30) Tai, S., Sun, Y., Squires, J. M., Zhang, H., Oh, W. K., Liang, C.-Z., and Huang, J. (2011) PC3 is a cell line characteristic of prostatic small cell carcinoma. *Prostate 71*, 1668–1679.

(31) Alimirah, F., Chen, J., Basrawala, Z., Xin, H., and Choubey, D. (2006) DU-145 and PC-3 human prostate cancer cell lines express androgen receptor: Implications for the androgen receptor functions and regulation. *FEBS Lett. 580*, 2294–2300.

(32) Rapozzi, V., and Jori, G. (2015) Resistance to Targeted Anti-Cancer Therapeutics. *Resistance to Photodynamic Therapy in Cancer Volume 5* (Rapozzi, V., and Jori, G., Eds.) pp. 3–26, Chapter 1, Springer Press.

(33) Robey, R. W., Steadman, K., Polgar, O., Morisaki, K., Blayney, M., Mistry, P., and Bates, S. E. (2004) Pheophorbide a is a specific probe for ABCG2 function and inhibition. *Cancer Res. 64*, 1242–1246.

(34) Robey, R. W., Steadman, K., Polgar, O., and Bates, S. E. (2005) ABCG2-mediated transport of photosensitizers: Potential impact on photodynamic therapy. *Cancer Biol. Ther. 4*, 187–194.

(35) Selbo, P. K., Weyergang, A., Eng, M. S., Bostad, M., Mælandsmo, G. M., Hogset, A., and Berg, K. (2012) Strongly amphiphilic photosensitizers are not substrates of the cancer stem cell marker ABCG2 and provides specific and efficient light-triggered drug delivery of an EGFR-targeted cytotoxic drug. *J. Control. Release 159*, 197–203.

(36) Ingram, W. J., Crowther, L. M., Little, E. B., Freeman, R., Harliwong, I., Veleva, D., Hassall, T. E., Remke, M., Taylor, M. D., and Hallahan, A. R. (2013) ABC transporter activity linked to radiation resistance and molecular subtype in pediatric medulloblastoma. *Exp. Hematol. Oncol. 2*, 26-43.

(37) Bessho, Y., Oguri, T., Achiwa, H., Muramatsu, H., Maeda, H., Niimi, T., Sato, S., and Ueda, R. (2006) Role of ABCG2 as a biomarker for predicting resistance to CPT-11/SN-38 in lung cancer. *Cancer Sci. 97*, 192–198.

(38) Castoria, G., D'Amato, L., Ciociola, A., Giovannelli, P., Giraldi, T., Sepe, L., Paolella, G., Barone, M. V., Migliaccio, A., and Auricchio, F. (2011) Androgen-induced cell migration: role of androgen receptor/filamin A association. *PLoS One 6*, e17218.

(39) Tesei, A., Leonetti, C., Di Donato, M., Gabucci, E., Porru, M., Varchi, G., Guerrini, A., Amadori, D., Arienti, C., Pignatta, S., et al. (2013) Effect of Small Molecules Modulating Androgen Receptor (SARMs) in Human Prostate Cancer Models. *PLoS One 8*, e62657.

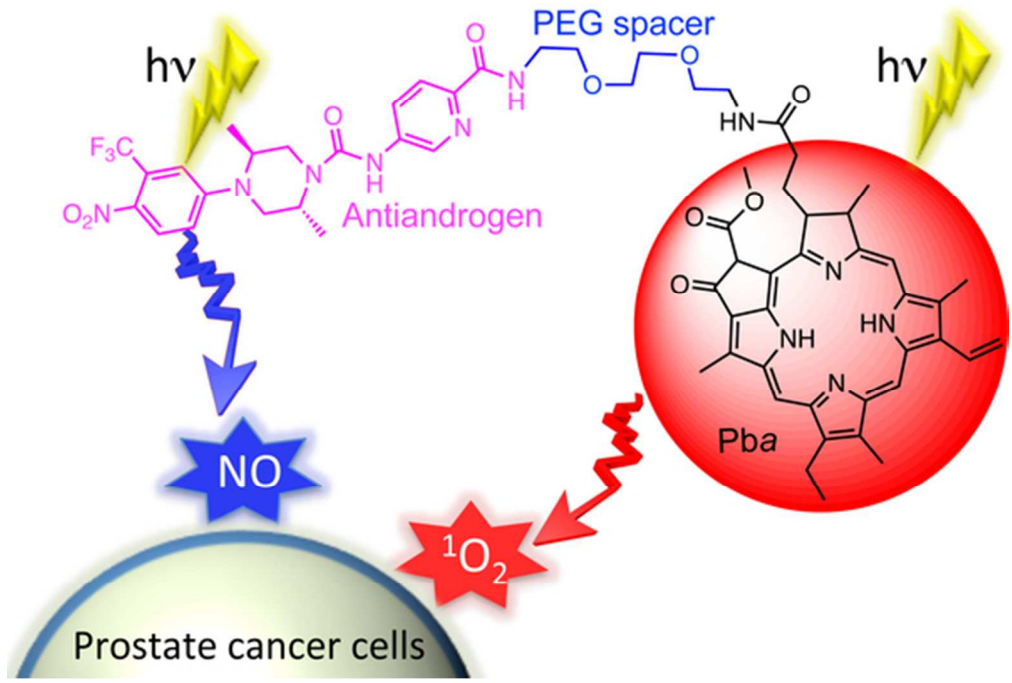

50x34mm (300 x 300 DPI)

28x9mm (300 x 300 DPI)

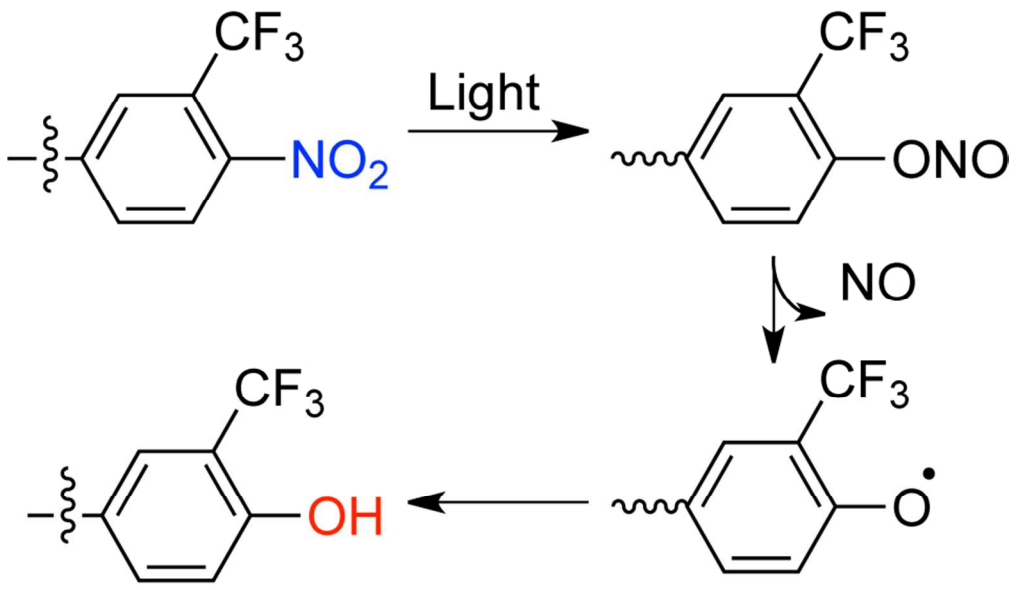

81x47mm (300 x 300 DPI)

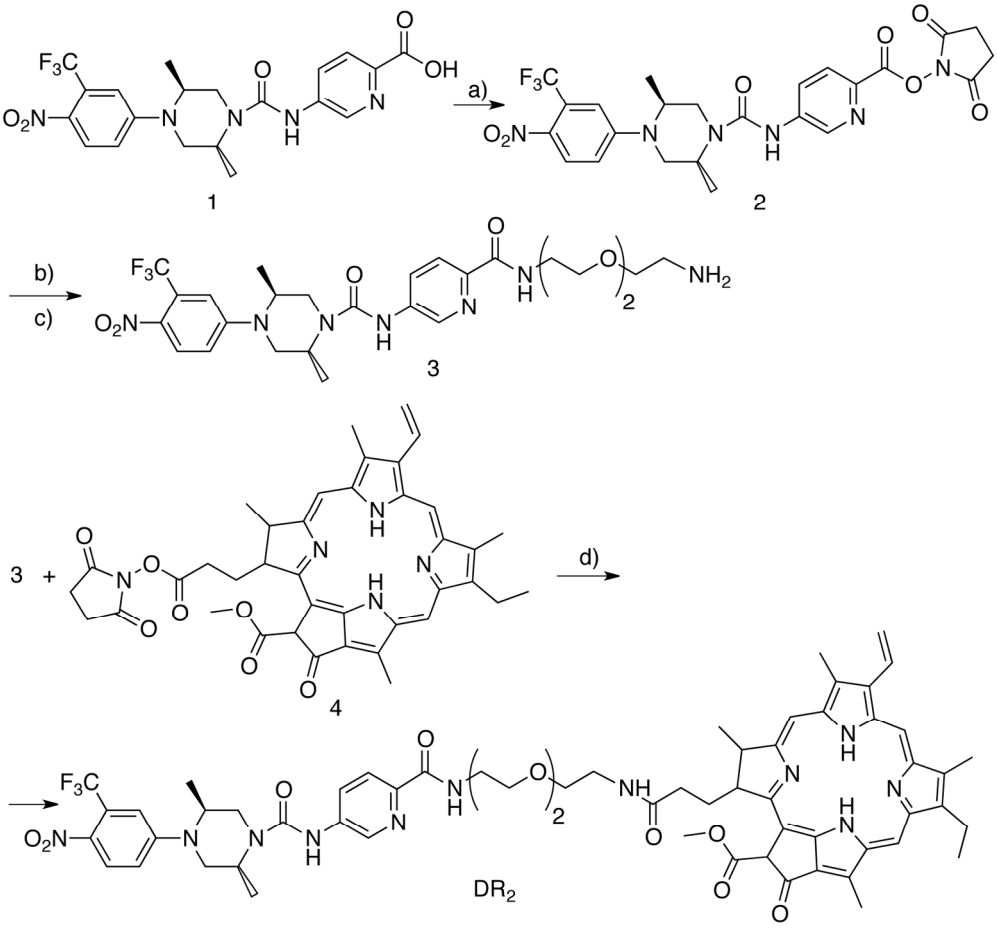

154x144mm (300 x 300 DPI)

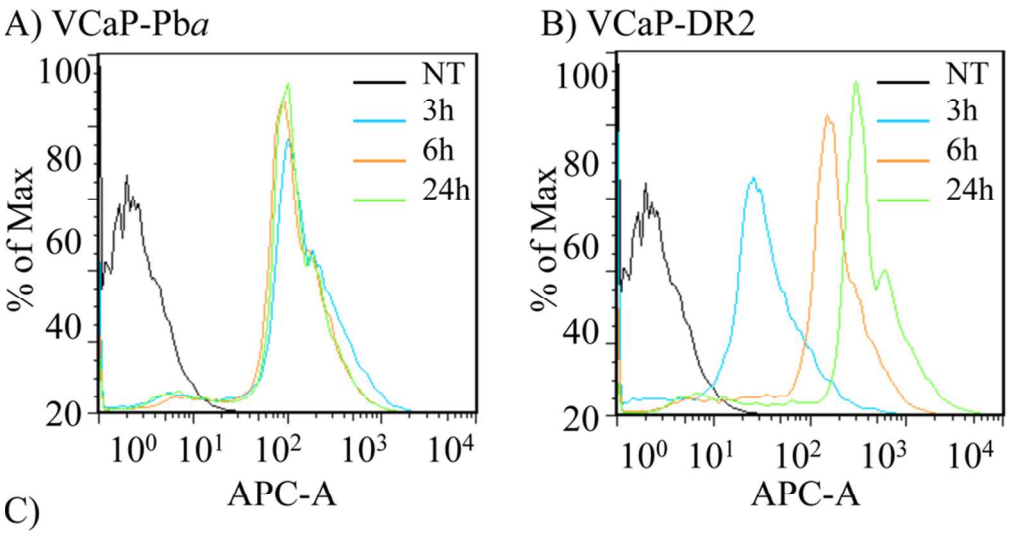

C)

	3h	6h	24h		3h	6h	24h
Pb*a* (1 µM)	188.9	142	144	**DR2** (1 µM)	46.6	206	486

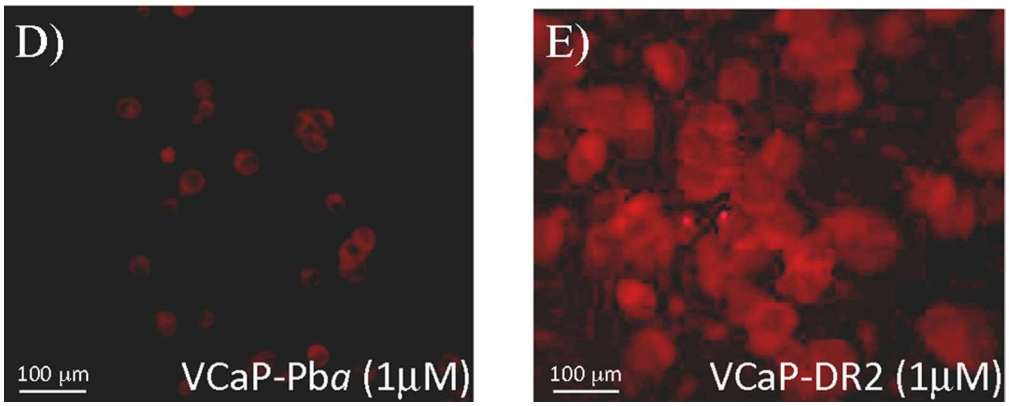

84x91mm (300 x 300 DPI)

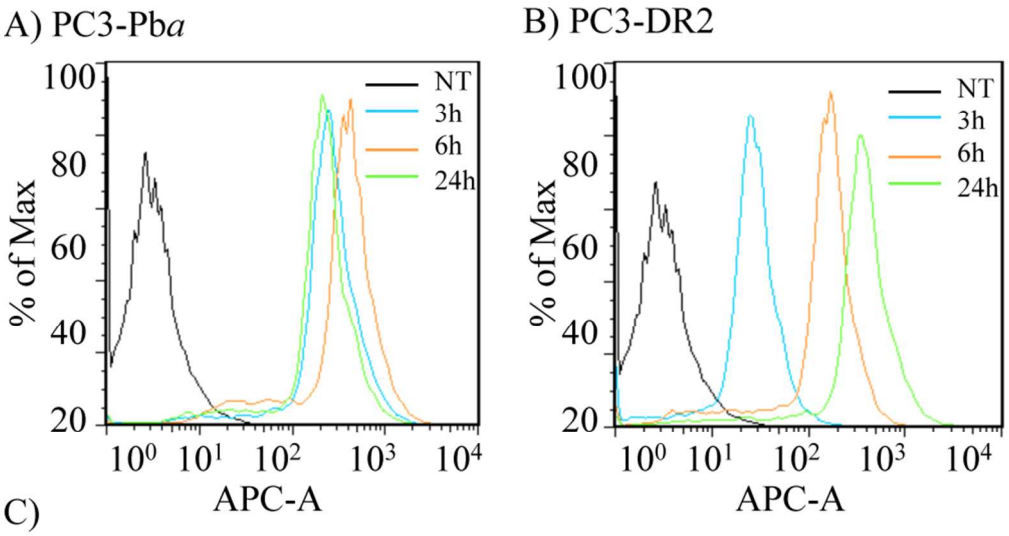

C)

	3h	6h	24h		3h	6h	24h
Pb*a* (1 μM)	302.9	429	249	**DR2** (1 μM)	30.6	170	422

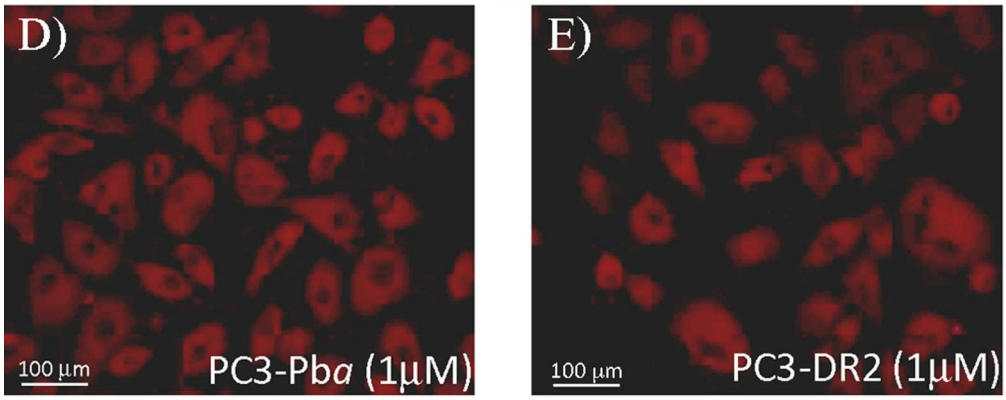

84x89mm (300 x 300 DPI)

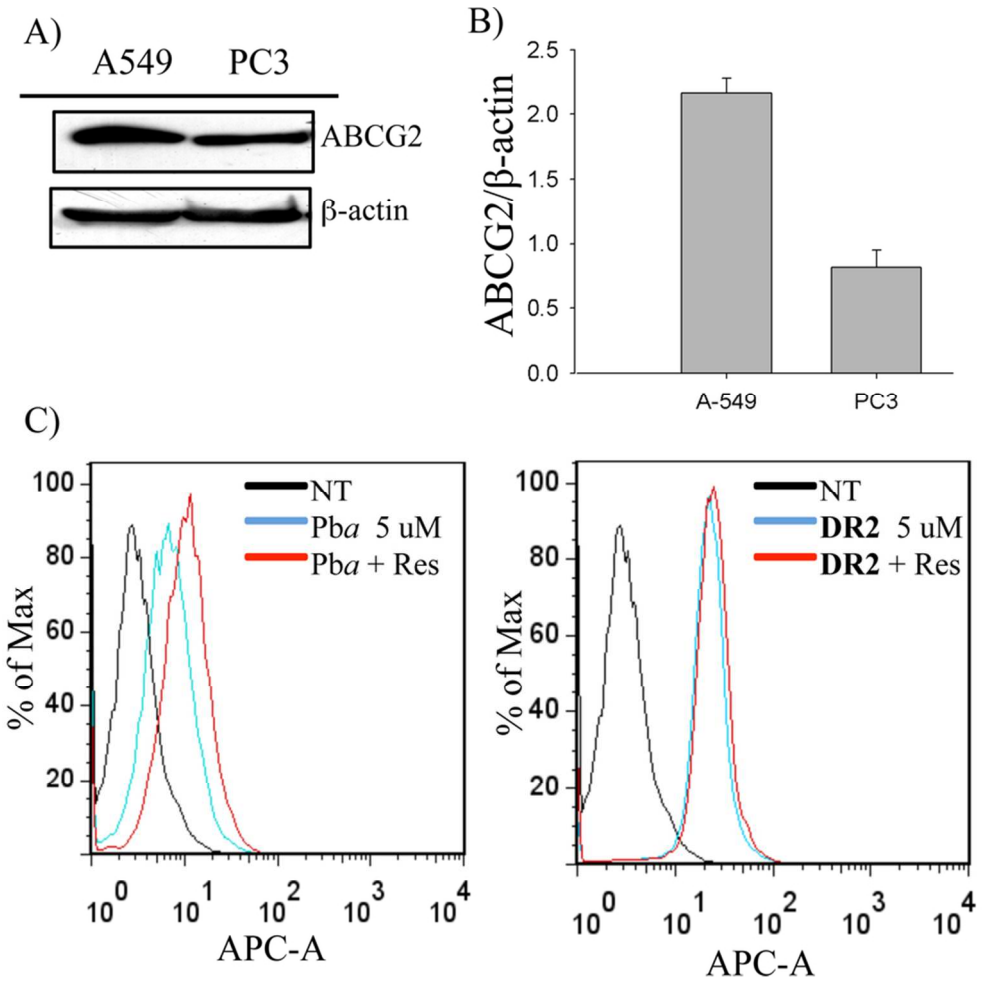

81x79mm (300 x 300 DPI)

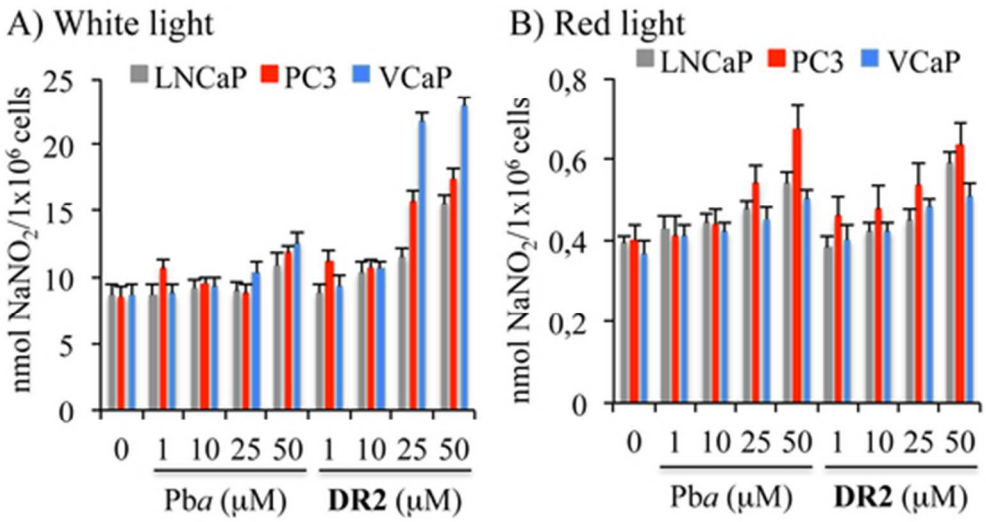

45x24mm (300 x 300 DPI)

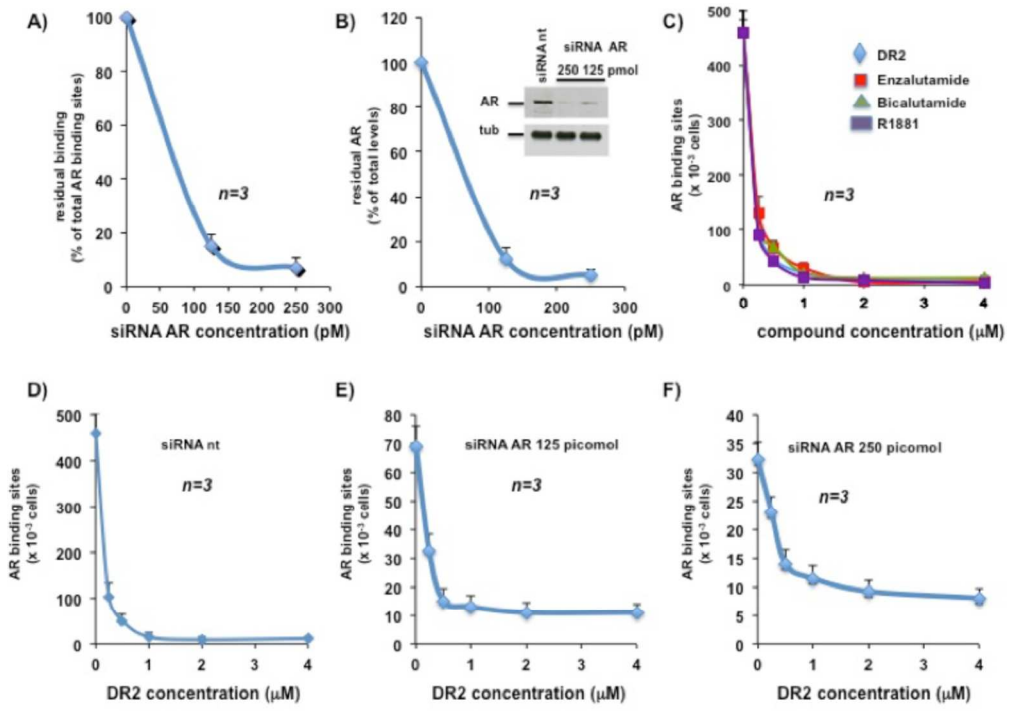

125x88mm (300 x 300 DPI)

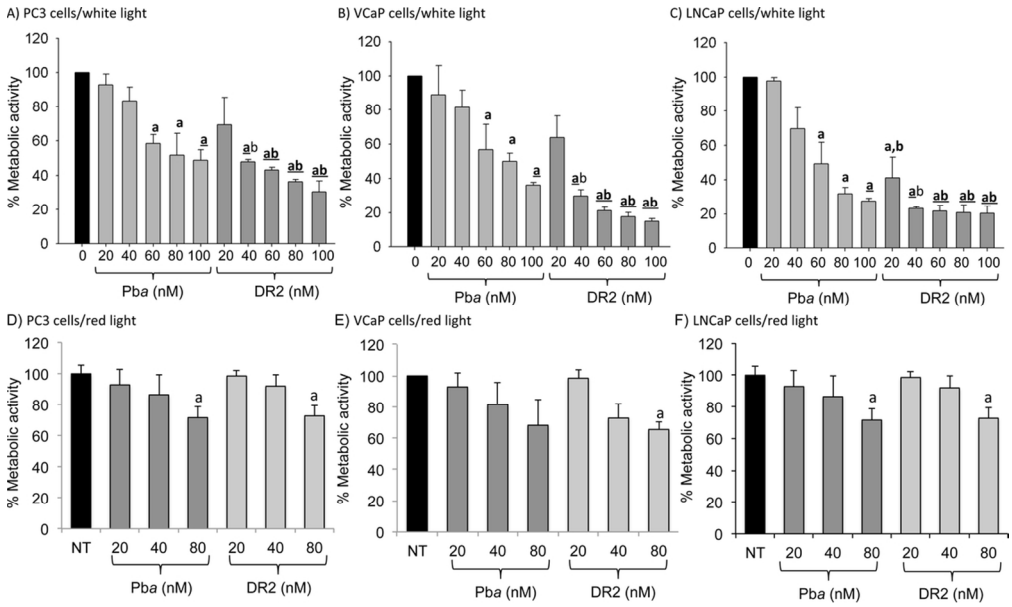

104x62mm (300 x 300 DPI)